21 December 1998

PHYSICS LETTERS A

ELSEVIER

Physics Letters A 250 (1998) 111–116

Velocity field measurements in granular gravity flow in a near 2D silo

A. Medina [a], J.A. Córdova [b], E. Luna [b], C. Treviño [b]

[a] *Subdirección de Exploración y Producción IMP, A.P. 14-805, 07730 Mexico D.F., Mexico*

[b] *Departamento de Fisica, Facultad de Ciencias, UNAM, A.P. 70-564, 04510 Mexico D.F., Mexico*

Received 30 June 1998; revised manuscript received 28 September 1998; accepted for publication 14 October 1998
Communicated by A.R. Bishop

Abstract

Using particle image velocimetry (PIV) we studied experimentally the whole velocity field during the discharge of monodisperse granular material from a flat-bottomed 2D silo. We have characterized important quantities of this flow such as the transversal flow oscillations, the mean velocity field and the velocity fluctuations. © 1998 Elsevier Science B.V.

PACS: 46.10.+z; 05.40.+j
Keywords: Mechanics of discrete systems; Fluctuation phenomena

1. Introduction

Experimentally it has been observed that, like in an hourglass, a silo filled with sand or other dry granular material induces a gravity flow which commonly exhibits, at several time scales, both regular and intermittent behavior in some relevant quantities. A regular behavior appears, for example, in the mass flow rate, which is a time-averaged quantity maintaining a value approximately constant during the discharge of a tall enough silo [1]. The intermittent patterns in this flow, as has already been noticed, should display fractal noise with a long-range time correlation in the number density near the exit [2–4] and in the pressure at the walls [5]. Despite the importance and consequences of these phenomena, a set of governing equations is still lacking, which would let us obtain good agreement with experimental results for one or various of those phenomena in a wide range of the parameter space. Perhaps the main difficulty in obtaining good agreement between theory and experiments is the discrete nature of grains having shocks, long-duration frictional contacts and, therefore, a complex mechanism of evolution of the translational and rotational kinetic energy.

During the flow, density fluctuations seems to occur around a mean value (see for example Refs. [1,3]) and therefore several experimental and theoretical efforts have been directed mainly to the knowledge of the velocity within the flow region [1,6–16]. Despite these restrictions, very few of those theoretical studies have shown an analysis of the whole velocity field in the steady-state flow [14] or in the time-dependent flow [11,15]. In this sense, the experimental evaluation of the velocity is necessary in order to obtain quantitative information of this gravity induced flow.

To get more precise knowledge of the structure of the granular flow, at least in an idealized geometry, we

PII S0375-9601(98)00795-6

present in this work an experimental study of the velocity field in a near two-dimensional silo (2D). This study is carried out in a zone close to the exit hole of a flat-bottomed silo. Our measurements let us show a series of experimental results, mainly related to the non-steady granular flow and its spatial and temporal fluctuations. In the next section we describe the experimental set-up for the velocity-field measurements and discuss the experimental procedure and the main aspects of the measurements nature. In Section 3 we perform the data analysis. We show that the whole velocity field has very interesting and complex dynamical properties. More specifically, we characterize the main frequency associated with the global transverse oscillations of the velocity field, the intensity of the velocity fluctuations and the mean of the velocity components for several heights from the bottom. Finally, in Section 4 we give the main conclusions and limitations of this work.

2. Experimental set-up and image processing

In this work we report on measurements of the velocity field in a wide zone of the flow at the lower part of a 2D silo. Experiments were performed in a vertical glass-walled silo of 100 cm height, $W = 30.0$ cm width and 3.8 mm deep filled up to $H = 82$ cm with monodisperse granular material composed of spherical glass beads with mean diameter $d = 3.15 \pm 0.04$ mm, mean friction static coefficient $\mu = 0.57$ and grain density $\rho_p = 2.45$ g/cm^3. In our experiments the ratio of the thickness of the silo to the particle diameter is close to 1.2 assuring a monolayer of (no overlapping) grains. During gravity flow the grains pass through a bottom exit with a size $D = 2$ cm, which was located just at the center. Fig. 1 shows the schematics of the experimental set-up.

When the exit hole was opened, the induced granular flow was recorded using a fast-shutter-speed (1/500 s) CCD camera with a recording frequency of 30 frames per second. A typical time elapsed for the main flow was around 25 s (i.e. 750 frames) but in order to analyze the main flow (and not initial transient phenomena) we have only taken into account frames recorded 5 s after the exit was opened. After, each recorded frame was digitized and fed to a computer as a digital image with a 256-gray scale each 1/30 s.

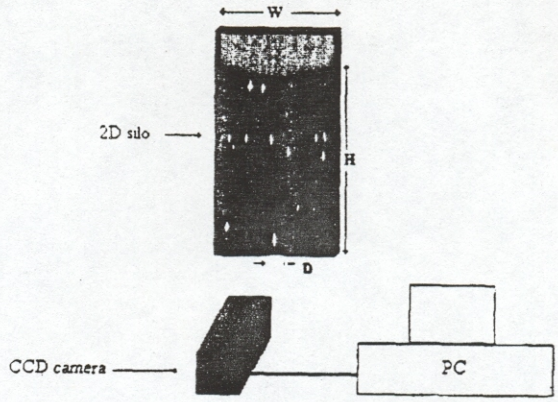

Fig. 1. Experimental set-up and geometrical parameters of the silo.

In order to obtain the velocity field we employed the particle image velocimetry (PIV) technique by using the commercial Insight TSI software. The PIV technique consists basically in determining the distance that particles have moved in the time elapsed between two consecutive digitized images [17]. Having each frame, it is then interrogated around a location $\boldsymbol{x} = (x, y)$, named the interrogation region (a small area with approximately 10 or more pairs of grains), and analyzing the vectorial displacements $\Delta \boldsymbol{x}$ of the particle image pairs within this region. By successively interrogating the frame at many adjacent interrogation regions, the particle velocity vector $\boldsymbol{v}$ in the plane of flow may be inferred at many positions in the flow field as $\Delta \boldsymbol{x}(\boldsymbol{r}) = \boldsymbol{v} \Delta t M$, where M is the image magnification factor, $\Delta t = 1/30$ s is the time interval between images (frames), and $\boldsymbol{r} = (x', y')$ refers to the particle position in the flow plane at a given time t.

Provided the particle image density is sufficiently high and the interrogation regions on the frame sufficiently small, the measured components of the velocity field vector may be considered nearly continuous over the field of view. Here, we have taken into account the whole measurement zone of the 2D granular flow having a size 30 cm height by 30.0 cm width (equal width that the silo). This zone can also be expressed as having an area of 542 × 542 pixels. The interrogation areas were varied from squared interrogation areas with size 32 × 32 pixels (around 18 pairs of grains) until squared interrogation areas with size 64 × 64 pixels (around 50 pairs). We obtain similar results for the velocity vectors and other important quantities using both measurement windows. The

magnification factor had a value of $M = 1.328$. The number of interrogation areas along the x (transverse) and y (longitudinal) directions must be large enough to obtain a good resolution of the velocity field.

In order to measure accurately the particle displacement in the interrogated area, the power spectrum of the digitized image is treated as a Young fringe pattern. More exactly, because the very small distance between two or more particle images and the high number of particle image pairs, it is possible to perform on each interrogation area an optical Fourier transform and then obtain an averaged measure of the particle displacement. The fringe patterns can be sampled along one or more pairs of orthogonal directions and then the corresponding spatial frequencies can be evaluated. The orthogonal projection of centroids is realized by first substituting each particle image with one pixel centered in its own centroid. The single pixels have all the same gray level. The values of every column and of every row of the new image are then summed up in order to obtain its x and y projections. The results of summations are arranged in order in two different linear arrays. The measurement of the mean particle displacement is then reduced to the analysis of the mean centroid displacement along two axis. This can be done by estimating the corresponding power spectrum. The information concerning the mean particle displacement in a certain direction can also be determined by estimating the wave number of the centroids along the same direction. This can performed by the corresponding power spectral density function. To get an accurate measurement we will note that the fringe spacing is inversely proportional to the mean value of particle displacement. Under these conditions the errors primarily results from the uncertainty in determining the centroids of the particles, producing in our case errors in the velocities around 1% [18].

3. Whole velocity field and its properties

3.1. Velocity field and transversal oscillations

With the experimental technique described in the previous section, we study the non-stationary flow and its mean properties, in order to gain some insight of their relevant aspects. Clearly, the description of the average motion of the grains in the interrogation area it is given in an Eulerian frame, because the interrogation areas are centered at the same points ($\boldsymbol{x}$'s) of the silo when the interrogation area and the number of these areas are fixed. For each consecutive pair of frames we obtained an space-averaged velocity vector $\boldsymbol{v} = (u(t), v(t))$ at a fixed position (the center of the interrogation area) and therefore the whole velocity field. Here, u and v are the horizontal and vertical components of velocity. In this work we have chosen between 10 and 50 of these overlapping interrogation areas along each direction. It means that we have a spatial resolution from 10×10 to 50×50 velocity vectors in the whole velocity field. In Fig. 2 we show, as a particular case, a whole velocity field of 30×10 velocity vectors (30 vectors along the x-axis and 10 vectors along the y-axis). We will also note that important differences in all quantities derived from the velocity vectors were not obtained by changing the number of interrogation areas.

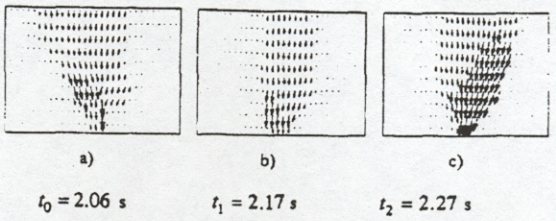

Fig. 2. Whole velocity field during gravity flow. (a) Main flow close to the left-hand side wall at time $t_0 = 2.06$ s. (b) Main central flow around $t_1 = 2.17$ s. (c) Main flow close to the right hand side around $t_2 = 2.27$ s. These plots show graphically the existence of an oscillation in the flow.

As an example of the unsteady structures detected in the velocity field, in Fig. 2 we show three snapshots of it obtained at different times but within a lapse of time of half a second, by using PIV data analysis. Here, the characteristic transversal typical oscillations are easily shown. Figs. 2a and 2c show the velocity vectors for non-symmetrical flow, where the main core of flow is towards the left and right, respectively, while Fig. 2b shows the case for almost symmetrical flow. These oscillations were obtained in all experimental runs with the peak around 2.4 Hz. In order to evaluate the main frequency of these oscillations we have obtained the power spectra of a relevant quantity (Fourier transform of the autocorrelation function). In fact, these power spectra (at several heights) have been obtained for the function $G(t)$ given by

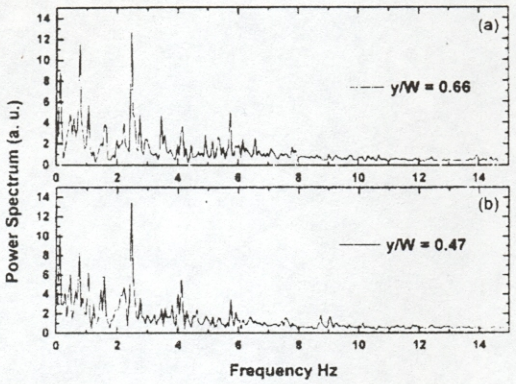

Fig. 3. Power spectrum (in arbitrary units) of the function $G(t)$ for two dimensionless heights. (a) $y/W = 0.66$ and (b) $y/W = 0.47$. Note the most important peak around $f_c \simeq 2.4$ Hz in both plots.

$$G(t) = X - \langle X \rangle, \tag{1}$$

where

$$X = \frac{1}{N\overline{v}} \sum_{i=1}^{N} x_i v_i, \tag{2}$$

and N corresponds to the number ($N = 30$ in our case) of data points i at a given height and x_i is the value of x at node i measured from the left wall of the silo. Here $\overline{v}(t) = (\sum_{i=1}^{N} v_i)/N$ denotes the spatial-averaged vertical velocity, while $\langle\ \rangle$ denotes a time-averaged quantity. Also, from Eq. (1) we found that $\langle G(t) \rangle = 0$.

An order of magnitude estimate gives that the characteristic velocity at the exit is of order $v_E \sim \sqrt{gD}$, while the characteristic velocity far above it must be of the order $v \sim \sqrt{gD^3}/W$, by using mass conservation. In our case $v_E \sim 40$ cm/s and $v \sim 3$ cm/s. The frequencies associated are of order $f_E \sim \sqrt{gD}/D \sim 20$ Hz and $f \sim \sqrt{gD^3}/W^2 \sim 0.1$ Hz. This large disparity in the frequencies involves a large number of characteristic times in the flow process. However, due to the global structure of the induced oscillations, a preferred frequency can be obtained from the power spectra of $G(t)$. Fig. 3 shows typical power spectra at two different heights $y/W = 0.66$ (Fig. 3a) and 0.47 (Fig. 3b) from the bottom. We can see a series of peaks at relatively low frequency, showing the importance of the large scales induced far above the exit in this global mechanism. The main peak is found to be close to $f_c \simeq 2.4$ Hz at both heights. These changes in the main flow direction have been detected previously during the discharge from a flat-bottomed silo, of an idealized granular material composed of big acryl rods of equal radius [7].

These characteristic oscillations of the velocity field can also be associated directly to a Strouhal number. In this case we can define the Strouhal number as $\mathrm{St} = f_c W/\sqrt{gD}$, where f_c is a characteristic frequency of the flow. Therefore, with this definition of the Strouhal number we obtain at the main peak $\mathrm{St} \simeq 1.6$. In general the Strouhal number must be a functional of the form

$$\mathrm{St} = \Phi(D/W, d/D), \tag{3}$$

which could be obtained experimentally. Despite the oscillations the flow is, on average, symmetric. This situation is noted visually in the central depression of the free surface during flow.

3.2. *Mean flow and fluctuations*

In practical terms it is possible to obtain the velocity field v of a *non-steady* flow as the sum of a mean or time-averaged velocity field $\langle v \rangle$ plus the fluctuating velocity field v', i.e. $v = \langle v \rangle + v'$ such that $\langle v' \rangle = 0$ [19]. The intensity of the velocity fluctuations are basically represented by the root mean square (rms) of v', normalized with the mean velocity and are represented in the main components (Tu, Tv) as

$$(Tu, Tv) = \left(\frac{\langle u'u' \rangle^{1/2}}{\langle u \rangle}, \frac{\langle v'v' \rangle^{1/2}}{\langle v \rangle} \right). \tag{4}$$

In Fig. 4 we show the plot of Tu (Fig. 4b) and Tv (Fig. 4a) as a function of the x/W for three different dimensionless heights ($y/W = 0.21$, $y/W = 0.47$, and $y/W = 0.66$) from the bottom. These patterns are typical of turbulent flow [19] (although the form of these patterns is not the best or even the unique signal of its existence) and their form is qualitatively maintained for all the heights. Here, we show that Tu has a maximum just at the center and also has minimum values symmetrically around the center. This maximum value is due to the very low value of the mean velocity close to the center plane. A different situation occurs in case of Tv, where the lowest values of the root mean square of the fluctuations are smaller close to the center plane. In these regions, the fluctuation

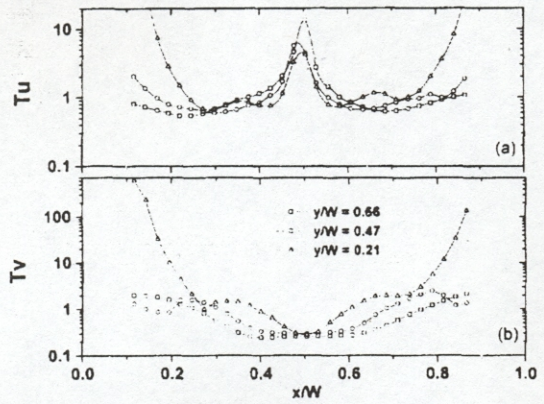

Fig. 4. RMS of the velocity fluctuations related to the mean velocity for three dimensionless heights. (a) Transversal component; (b) vertical component.

intensity is around half of the mean horizontal velocity component. The ratio of the silo width to the exit size in our case is $W/D \simeq 15$.

The time-averaged velocity profiles normalized with $\sqrt{gD}$ are shown in Fig. 5 at three different dimensionless heights from the bottom, obtained on a period of 20 s approximately. In Fig. 5a we show the horizontal component while in Fig. 5b the vertical velocity component is shown. In essence the structure of these patterns does not change with the height. The data behavior is very similar to that reported previously elsewhere [1], showing the reliability of our experimental method. In some previous experiments, the kinematic model [1] showed a better fit. Here the velocity profiles were well fitted by the correlations obtained through this model, i.e.

$$\langle \hat{v} \rangle = \langle \hat{v}_0 \rangle \exp\left(- \frac{(\hat{x} - 1/2)^2}{4B\hat{y}} \right), \tag{5}$$

and

$$\langle \hat{u} \rangle = -B \frac{\partial \langle \hat{v} \rangle}{\partial \hat{x}} = \frac{\langle \hat{v}_0 \rangle (\hat{x} - 1/2)}{2\hat{y}} \exp\left(- \frac{(\hat{x} - 1/2)^2}{4B\hat{y}} \right), \tag{6}$$

where $\langle \hat{v}_0 \rangle$ is the dimensionless average vertical velocity (normalized by $\sqrt{gD}$) just at the center of the silo, B is a dimensionless fitting parameter (normalized by W) and $\hat{x} = x/W$, $\hat{y} = y/W$. Additionally, $\hat{v} = v/\sqrt{gD}$ and $\hat{u} = u/\sqrt{gD}$. The coordinate y was measured from the bottom of the silo. Like other authors [1,13] we also have found that the kinematic parameter B changes with the dimensionless height in a non-linear form (Fig. 6). However, in the measurement range, the parameter B depends on $\hat{y}$ as

$$B \simeq 0.007 \exp(2.6\hat{y}). \tag{7}$$

Computer simulations, named distinct element method (DEM), used to study the steady-state granular flow in

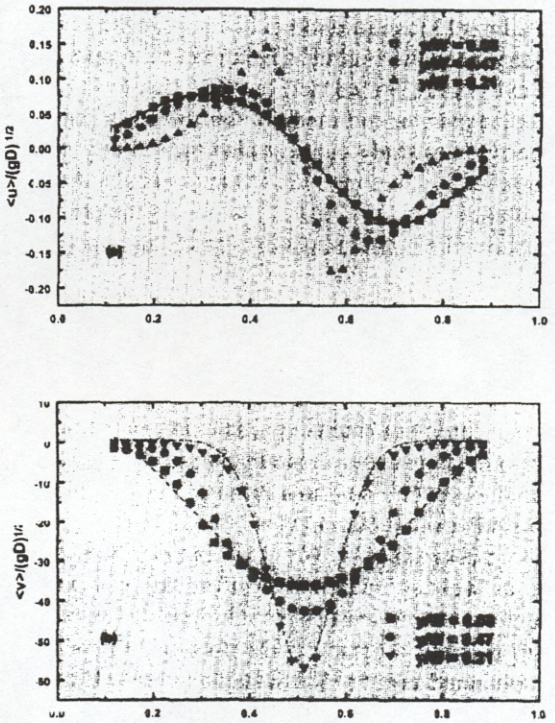

Fig. 5. Time-averaged velocity profiles at three different dimensionless heights. (a) Average profile and their fit (curves) for the transversal velocity. (b) Profile and their fit for the vertical velocity. The averaging was made in a period of 20 s.

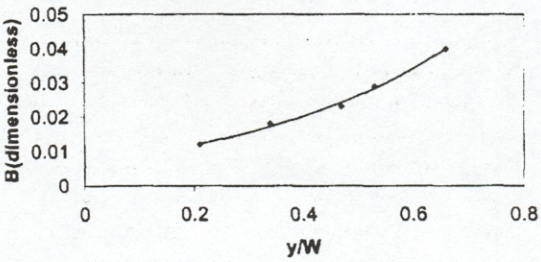

Fig. 6. Kinematic parameter B as a function of the dimensionless height $\hat{y} = y/W$.

flat silos [13], show another behavior in the parameter B very near the bottom. Experimental proofs of this behavior were not carried out here due to limitations of our experimental method. On the other hand, this experimental study can test also the validity of other computer simulations such as the molecular dynamics simulations (MDS) [10,11] which, at the present, do not show the complex patterns found in experiments.

4. Conclusions

In this work we used the non-intrusive technique of measurement named particle image velocimetry (PIV) to study experimentally the steady and unsteady granular velocity field in a 2D silo. In experiments we analyzed around 600 images in total, covering around 20 s at 30 frames/s. We also obtained both qualitative as well as quantitative information on the flow structure. In this sense, we could resolve velocity fluctuations from 0.05 to 15 Hz. In typical experiments we obtained around 600 instantaneous velocity vector plots, covering the whole area of interest in the silo's geometry. Using this information we have obtained the mean velocity and the fluctuation intensities given by the normalized root mean square of the fluctuating velocity field. We also have detected the existence of transversal flow oscillations with a very well associated frequency around 2.4 Hz. This mechanism is global in the sense that both the large spatial scale W and the small spatial scale D have important influences on this process. For the steady-state velocity field we have obtained a good agreement between the kinematic model and our experimental data for both $(\langle\hat{u}\rangle, \langle\hat{v}\rangle)$ velocity profiles. A very strong dependence of the parameter B on the dimensionless height was obtained when the exit size was kept fixed.

Finally, similar experimental studies of the granular flow in other geometries, i.e. other shapes of silo and in channels [20], are now very interesting and efforts in this direction are in progress.

Acknowledgement

This work has been supported by a grant from CONACyT-México under number 405P-E9506. We acknowledge Professor J. Andrade for his aid in the experimental work. We also acknowledge Professor E. Ramos and his group, for the support in using digitization software and equipment.

References

[1] U. Tuzun, G.T. Houlby, R.M. Nedderman, S.B. Savage, Chem. Eng. Sci. 37 (1982) 1691, and references therein.
[2] K.L. Schick, A.A. Verveen, Nature 251 (1974) 599.
[3] J. Andrade, C. Treviño, A. Medina, Phys. Lett. A 223 (1996) 105.
[4] C.T. Veje, P. Dimon, Phys. Rev. E 56 (1997) 4376.
[5] G.W. Baxter, R. Leone, R.P. Behringer, Europhys. Lett. 21 (1993) 569.
[6] A. Khelil, J.C. Roth, Eur. Jour. Mech. B/Fluids 13 (1994) 57.
[7] H. Sakaguchi, E. Ozaki, T. Igarashi, Int. J. Mod. Phys. B 7 (1993) 1949.
[8] R.L. Brown, J.C. Richards, Principles of Powder Mechanics (Oxford Univ. Press, Oxford, 1970).
[9] R.M. Nedderman, Statics and Kinematics of Granular Materials (Cambridge Univ. Press, Cambridge, 1992).
[10] G.H. Ristow, J. Phys. (France) I 2 (1992) 649.
[11] D.C. Hong, J.A. McLennan, Physica A 187 (1992) 159.
[12] D. Hirshfeld, Y. Radzyner, D.C. Rapaport, Phys. Rev. E 56 (1997) 4404.
[13] K.D. Kafui, C. Thornton, Some observations on granular flow in hoppers and silos, in: Powders and Grains 97, eds. R.P. Behringer, J.T. Jenkins (Balkema, Rotterdam, 1997) p. 511.
[14] F. Wang, C. Gardner, D.G. Schaeffer, SIAM J. Appl. Math. 52 (1992) 1076.
[15] U. Haüssler, J. Eibl, J. Eng. Mech. 110 (1984) 957.
[16] L. Srinivasa Mohan, P.R. Nott, K. Kesava Rao, Chem. Eng. Sci. 52 (1997) 913.
[17] P. Buchhave, Particle Image Velocimetry – Status and Trends, in: Experimental Heat Transfer, Fluid Mechanics and Thermodynamics 1991. eds. J.F. Keffer, R.K. Shah, E.N. Ganic (Elsevier, Amsterdam, 1991) p. 35.
[18] L. Lourenco, A. Krothapalli, Exp. Fluids 18 (1995) 421.
[19] W.D. McComb, The Physics of Fluid Turbulence (Oxford Univ. Press, Oxford, 1992).
[20] V.V.R. Natarajan, M.L. Hunt, E.D. Taylor, J. Fluid Mech. 304 (1995) 1.